



PKPD of PLGA-PEG-PLGA Copolymeric Micelles

15

Shirleen Miriam Marques and Lalit Kumar

Contents

1	Introduction	274
2	Synthesis and Purification of PLGA-PEG-PLGA Copolymer	274
3	Characterization of PLGA-PEG-PLGA Triblock Copolymer	275
4	Factors Affecting the Formation and Characteristics of the PLGA-PEG-PLGA Copolymeric Micelles	277
5	Pharmacokinetics (PK) and Pharmacodynamics (PD) of Copolymeric Micelles Based on PLGA-PEG-PLGA	279
6	Conclusion	288
	References	289

Abstract

Much research has been undertaken on stimuli-sensitive polymers and their applications in biochemistry, biomedicine, and a plethora of domains over the last decade. Stimuli-sensitive gelling polymers or in situ forming hydrogels, in particular, have drawn a lot of interest as prospective injectable implant systems with low invasiveness. Drugs or cells can be readily combined with the aqueous copolymer solution at low temperatures, and then injected into the body at a specific spot to form a semisolid

matrix. Nanoparticles composed of amphiphilic block copolymers with biodegradable core-forming blocks are extremely appealing for the development of long-acting drug delivery systems. The FDA-approved PLGA-PEG-PLGA triblock copolymer possesses the capability to provide sustained release of various biologicals. Polymer solutions having an ability to convert from sol to gel at physiological temperatures can be used for in situ gel formation and injectability. Drug delivery systems with more complicated architectures are being developed as technology advances. As a result, the processes of drug absorption and disposition following the administration of these newer delivery systems have grown extremely complicated. Thus, knowledge of the pharmacokinetics and pharmacodynamics could be

S. M. Marques · L. Kumar (✉)
Department of Pharmaceutics, Manipal College of
Pharmaceutical Sciences, Manipal Academy of
Higher Education, Manipal, Udipi, Karnataka, India
e-mail: lalit.kumar@manipal.edu

utilised to disentangle these complexities and increase our understanding of these drug delivery systems' *in vivo* behaviour, hence guiding their preclinical-to-clinical translation and clinical development.

Keywords

PLGA-PEG-PLGA · Copolymeric micelle · Amphiphilic · Pharmacokinetics · Pharmacodynamics · Hydrogel

1 Introduction

The use of polymeric nanoparticles in medicine to achieve site-specific medication delivery has recently piqued interest. Polymeric micelles, in particular, are now recognised as one of the most potential transporters [1]. The polymer poly(lactide-co-glycolic acid) (PLGA) which has received approval from the FDA has been examined for its biocompatibility and toxicity [2, 3]. To lengthen the release period of linked pharmaceuticals, the D,L-lactide (LA) to glycolide (GA) ratio, molecular weight, and hydrophilic properties of the polymer can be adjusted. The release of the drug in a controlled manner, reduced cytotoxicity, and few adverse events have all been demonstrated with PLGA nanoparticles. When chemically attached to the PLGA block, polyethylene glycol (PEG) displays a sluggish removal from the circulation, thereby resulting in a greater drug release and reduced absorption of PLGA nanoparticles by the reticuloendothelial system in comparison to the non-conjugated PLGA [2].

PEG/PLGA [4, 5], PEG/poly(caprolactone) [6], PEG/poly(propylene glycol)/polyester, PEG/peptide [7, 8] and poly(phosphazenes) [9, 10] are examples of biodegradable thermoresponsive copolymers that undergo sol-gel transitions in water when the temperature rises [11]. Self-assembled nano-micelles composed of the amphiphilic PEG and PLGA copolymers are used for the incorporation of hydrophobic as well as hydrophilic medicines and offer prolonged release of the therapeutic cargo [12]. Unlike poloxamer copoly-

mers, which have an exterior hydrophilic block, this block copolymer has hydrophilic inside blocks, which results in a distinct gelation mechanism. In this instance, gelation is likely to occur via flower-like micelle aggregation and the creation of an irregular percolated network [13]. In water, copolymers made up of hydrophobic and hydrophilic segments result in the formation of micelles, reducing free energy mostly due to hydrophobic interactions [14].

The release of drugs from these copolymers is accomplished by the following mechanisms: (i) diffusion of the drug present in the hydrogel during the early release period, and (ii) release of the drug via hydrogel matrix erosion during the latter phase [15]. Poly(lactide-co-glycolide)-poly(ethylene glycol)-poly(lactide-co-glycolide) (PLGA-PEG-PLGAs) possessing water solubility at ambient temperature allows for easy cargo loading and injection administration. In addition, the structure of the gel might be able to safeguard and release the trapped drug in a controlled manner [16]. PLGA-PEG-PLGA (Fig. 15.1) displays properties of a possible thermogel matrix, demonstrating a less invasive method of transporting cells and bioactive compounds. At low temperatures (4 °C), the PLGA-PEG-PLGA copolymer dissolves in water, but the solution gels spontaneously at 37 °C as seen in Fig. 15.2 [17]. Due to its ease of synthesis, remarkable reproducibility, and widespread acceptance of safety, the thermosensitive and biodegradable PLGA-PEG-PLGA hydrogel has attracted a lot of attention. Triblock PLGA-PEG-PLGA polymer is a suitable choice for drug carriers because of its non-cytotoxicity, outstanding temperature sensitivity, outstanding biocompatibility, and biodegradability and have been used for various clinical applications as depicted in Fig. 15.3 [18, 19].

2 Synthesis and Purification of PLGA-PEG-PLGA Copolymer

Zentner et al. outlined a traditional ring opening method to synthesize the PLGA-PEG-PLGA copolymer [20]. An appropriate amount of PEG was added into a stainless steel reactor, and the

Fig. 15.1 Structure of PLGA-PEG-PLGA copolymer

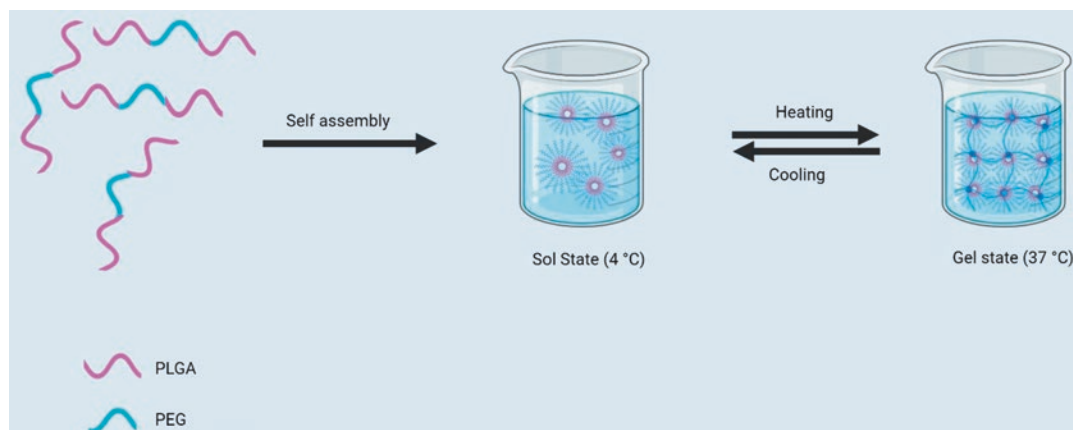
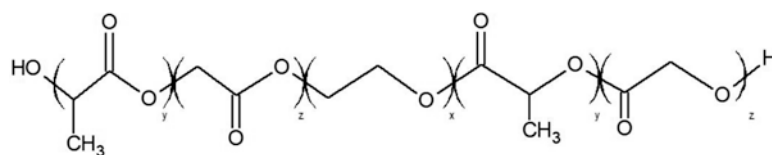


Fig. 15.2 Gelation mechanism of PLGA-PEG-PLGA copolymeric micelles

heating was carried out for 2 h at a temperature of 150 °C under 5 mmHg vacuum; after which, the desired quantities of LA and GA were loaded into the reactor. For 30 minutes, the reactor was operated at a temperature of 150 °C. A catalyst, stannous 2-ethylhexanoate, was introduced and was subsequently followed by heating the contents of the reactor at a temperature of 160 °C for duration of 6 hours below 5 mmHg vacuum [21–23].

In a study conducted by Yu and co-workers, the arrangement of the PLGA blocks in the copolymer of PLGA-PEG-PLGA was discovered to be influenced due to different polymerization conditions. Variations in the reaction affinity between LA and GA in ring opening polymerization, as well as post-polymerization transesterification, were blamed for the different arrangements in the triblock copolymer. The sol-gel conversion which was temperature induced in water was observed in an aqueous solution of the triblock copolymer. Moreover, the gelling behaviours could be adjusted by modifying the arrangement in the PLGA segment. The current research also revealed that the thermosensitive nature of the triblock copolymer was determined to be affected by the sequence structure present in the PLGA

segment. The transesterification in the polymerization process is primarily responsible for the differences in sequence structure among the copolymers. The balance in the hydrophobic and hydrophilic nature is altered by different sequence structures and polydispersities, which is essential for determining the micellization behaviour of these copolymers in water [24].

3 Characterization of PLGA-PEG-PLGA Triblock Copolymer

3.1 ¹H Nuclear Magnetic Resonance (NMR)

Copolymer structural analysis is crucial from both a theoretical and an industrial standpoint. In the study of copolymers, high-resolution NMR analysis is especially useful because it exposes structural and sequence information that cannot be deduced by other methods. NMR, especially ¹H NMR, is a simple and accurate method for determining copolymer composition, and it is generally more accurate than other conventional

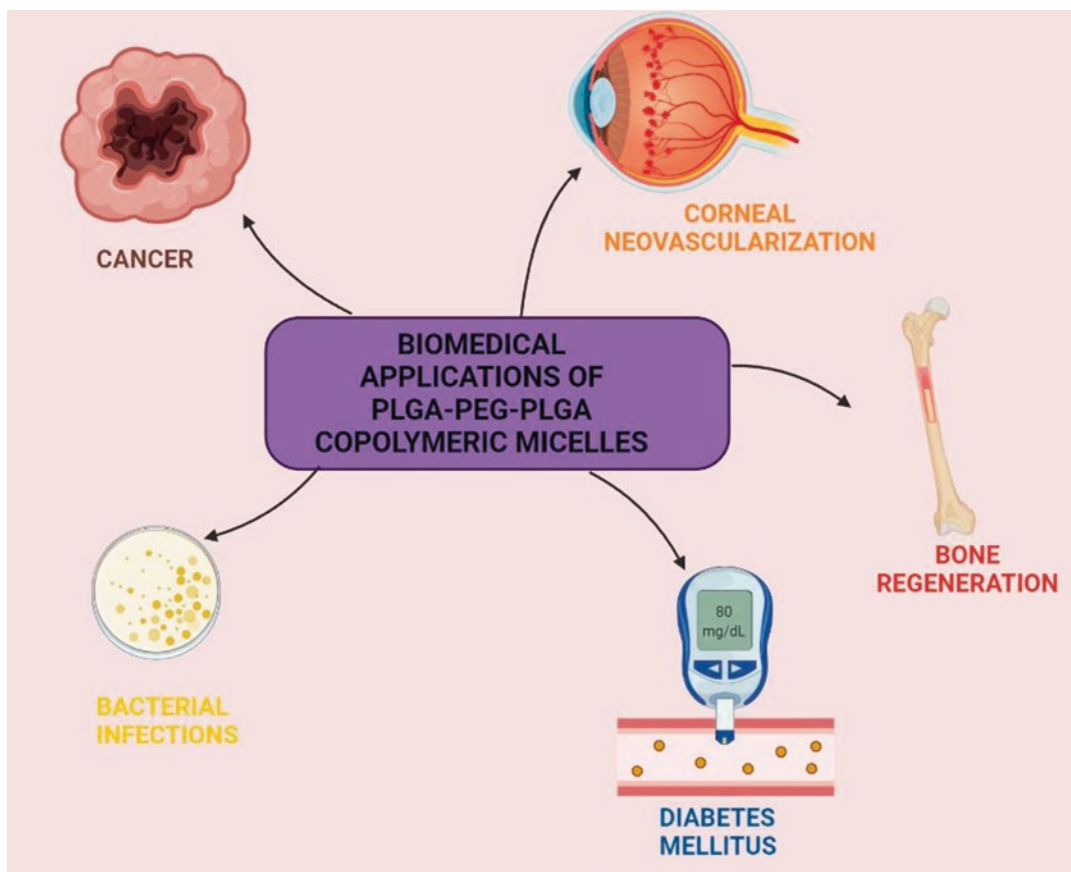


Fig. 15.3 Biomedical applications of PLGA-PEG-PLGA copolymeric micelles

analytical methods such as elemental analysis [25]. Ghahremankhani and group performed the structure analysis and estimation of molecular weight of the PLGA-PEG-PLGA copolymer using the ^1H NMR spectrum. Signals for PLGA-PEG-PLGA are found at = 5.1 ppm (a for CH of LA), 1.45 ppm (b for CH_3 of LA), 4.7 ppm (c for CH_2 of GA), 3.52 and 4.2 ppm (d and e for CH_2 of ethylene GA), and 3.52 and 4.2 ppm (d and e for CH_2 of ethylene glycolide) [26]. Similarly in order to elucidate the structure of the copolymers, determine the LA/GA ratio, and determine the number average molecular weight (M_n) of the PLGA-PEG-PLGA copolymers, ^1H NMR was performed by Khodaverdi and co-workers. The CH of LA, the CH_2 of GA, a CH_2 of PEG, another CH_2 of PEG, and the OH and CH_3 of LA, respectively, are the signals that appeared at 5.2, 4.8, 4.3, 3.5, 2.6, and 1.5 ppm. Moreover, the ratios of

the monomers that were used initially in the polymerization process matched very well with the LA-to-GA quantities which were calculated by ^1H NMR [27].

3.2 Gel Permeation Chromatography (GPC)

GPC was utilized to deduce information regarding the molecular weight and molecular weight distribution. In the study conducted by Chen and co-workers, the triblock copolymer was found to have a retention time of about 18 minutes, while the remaining two peaks in the chromatogram (retention time of about 21 minutes) were found to be of the solvent. Both copolymers were found to have a polydispersity of about 1.3, with a symmetric peak and a comparatively small

MWD. Further, the formation of the triblock polymer was confirmed by a single GPC trace along with a low polydispersity value [28].

3.3 Fourier Transform Infrared (FTIR)

FTIR spectroscopy is an important tool for determining the properties of both polymeric and biopolymeric materials. This technique has been effectively implemented for the assessment of polymerization process, characterization of the polymer structure, polymer surface, polymer degradation, and polymer modification, as well as in the identification and characterization of homopolymers, copolymers, and polymer composites [29]. The structure of PLGA-PEG-PLGA was validated by FTIR in a study done by Mohajeri and colleagues. The presence of both blocks can be seen in the FTIR spectrums of PLGA-PEG-PLGA at 1100 cm^{-1} (etheric C-O of PEG) and 1700 cm^{-1} (ester carbonyl of PLGA) [30]. The methods used for characterization of the triblock copolymer have been tabulated in Table 15.1.

4 Factors Affecting the Formation and Characteristics of the PLGA-PEG-PLGA Copolymeric Micelles

4.1 Molecular Weight Distribution (MWD) of PEG Block

MWD is among the most fundamental molecular properties of a synthetic polymer. The impact of the PEG block's MW and MWD on the micellization and phase transition of the PLGA-PEG-PLGA aqueous system was investigated by Chen and co-workers. PEG is a one-of-a-kind polymer because of its characteristics, particularly since its solubility in water and hydrophobicity rise with temperature. PEG has a chemical structure that encourages the creation of hydrogen bonds with water. The loss of water entropy can be credited to

Table 15.1 Characterization parameters for PLGA-PEG-PLGA polymer

Method	Analytical target	Reference
^1H NMR	Number-average molecular weight M_n and the molar composition	[31]
Gel permeation chromatography	Average molecular number (M_n), molecular weight (M_w), and M_w/M_n ratio (i.e. polydispersity index (PDI))	[32]
Fourier transform infrared	Functional group characterization	[33]
Differential scanning calorimetry	Glass transition temperature (T_g)	[34]

the extremely localised arrangement of the water molecules that surrounded the PEG chain. The hydrophilic PEG blocks are also found in the micellar corona of PLGA-PEG-PLGA, and in a dispersed sample, the micelle sizes may be heavily influenced by the longer PEG chains. As a result, larger micelles and looser micelle coronae emerged from a wider dispersion of PEG block. At low temperatures, a larger MWD of the PEG segment produced bigger copolymer micelles, and the resulting system which was concentrated was found to become viscous and even physically gelled [35]. A decreased solubility promoted the hydrophobic association-driven physical gelation. The samples with smaller MWDs physically gelled not just at lower concentrations but also at lower temperatures in our thermosensitive macromolecular system. This could be due to the fact that it has a higher local hydrophobicity. Because of the increased local hydrophobicity, the micelles were more stable, allowing them to maintain their gel state over a larger temperature range [36].

4.2 LA and GA Sequences in the PLGA Block

In general, the type of initiators used together with the transesterification process during ring opening polymerization, which results in a random arrangement of the monomer units in the polymer chains,

is known to influence the sequence structures of PLGA. Yu et al. created and characterised a couple of PLGA-PEG-PLGA copolymers in which the arrangement of the PLGA segment in the PLGA-PEG-PLGA triblock copolymers was modified by varied polymerization settings. Differences in reaction affinity between LA and GA in ring opening polymerization, as well as post-polymerization transesterification, were blamed for the different arrangement in the copolymers. The temperature-sensitive sol-gel conversion in water was seen in the aqueous system of the PLGA-PEG-PLGA triblock copolymers, and the gelling behaviours were shown to be controllable by modifying the arrangement in the PLGA segment. Different profiles of micellization behaviours were found as the temperature increased the copolymers, demonstrating that self-assembly of the PLGA-PEG-PLGA copolymers in water depended on the sequence structures [24].

4.3 Length of PEG Block

A study conducted by Khorshid and co-workers aimed to determine the effect of the length of the hydrophilic PEG segment on the structural changes of the PLGA-PEG-PLGA triblock copolymer during gelation. The length of the hydrophobic PLGA block was held constant in this study, whereas the length of the hydrophilic PEG block was changed ($n = 1000$ and $n = 1500$). The change was found to produce a profound effect on the phase behaviour of aqueous samples as well as the polymer structure in both dilute and semi-dilute solutions. The results of turbidity and viscosity studies on dilute copolymer solutions imply that loose intermicellar structures arise when the temperature is raised initially, after which there was species contraction and disintegration to micelles at elevated temperatures. Both copolymers exhibit a similar pattern of action; however, the properties of the copolymer with long PEG spacer appear at significantly higher temperatures [37].

4.4 LA/GA Ratio

Sulaiman and co-workers used a factorial design technique to evaluate the co-block polymer behaviour and properties of a nanopolymeric micelle which were affected by PLGA formation (constituent components ratio) and PEG concentration. With respect to the solubility behaviour, the solubility was found to be the maximum at the highest LA-to-GA ratio. In terms of the polydispersity index (PDI), a polydisperse system was favoured by the low LA-to-GA ratio, which produced two peaks in the particle size distribution. Conversely, with a high LA-to-GA ratio, a monodisperse system was seen. The variation in co-block length was the main driver of particle size distribution. Co-blocks with a longer length were found to produce larger particles than those with a shorter length [38].

In a study conducted by Qiao and group, the effect of the LA/GA molar ratio on release of the drug from the triblock copolymer hydrogel was determined, wherein 5-fluorouracil was chosen as the hydrophilic drug and indomethacin was chosen as the hydrophobic drug. The molar ratio of LA to GA was found to have a minor impact on drug release driven by diffusion, while it had a considerable impact on the release of the drug release which was governed by erosion of the hydrogel. The reason for this could be attributed to the drugs being distributed in various regions of the hydrogel. Indomethacin partitions into the hydrogel's hydrophobic PLGA region and just a little quantity into the PEG region, whereas the hydrophilic 5-fluorouracil partitions into the PEG region. The drug present in the hydrophilic region was released by diffusion via the hydrophilic channels of the hydrogel that were relatively less affected by changes in the LA/GA ratio, whereas the hydrophobic indomethacin dispersed within the PLGA region was released due to erosion of the hydrogel [23].

4.5 Effect of PEG/PLGA Ratio

In a study conducted by Cespi and group, a thorough investigation was conducted to characterise a panel of copolymers of PLGA-PEG-PLGA so as to determine their thermal characteristics in the solid state and the rheological properties of their aqueous solutions. As a result, 15 tri-block copolymers were produced as well as analysed, each with a different MW and hydrophobicity (PEG/PLGA ratio). The DSC analysis conducted for the aforementioned produced copolymers revealed that copolymers having a PEG/PLGA ratio less than 1 in which the percent of PLGA block is dominant have an amorphous solid form (PLGA-like copolymers). PEG-like copolymers, on the other hand, have lower T_g values (-35°C), with crystallization and melting events ranging from -25°C to 0°C and 10°C to 35°C . Also at greater PEG/PLGA ratios, M_n has a noticeable effect on rheological characteristics. Copolymers that possess a PEG/PLGA ratio of 0.4 to 1 are either fully or partially hydrated, resulting in complete or partial thermogelling, or sol dispersions, depending on the structural features of the copolymers (PEG/PLGA ratio and M_n), at least up to a M_n of 8 kDa. The dispersions which had a M_n of 5 kDa and 5.9 kDa, respectively, and a PEG/PLGA ratio of 0.43 and 0.51, displayed thermogelling behaviour, thus verifying the restricted window of MW and PEG/PLGA ratio where thermogelling systems in aqueous solutions can be generated, irrespective of the concentration [39]. Gelling temperature and release of a model drug were tested by Steinmann and co-workers using triblock copolymers of PLGA-PEG-PLGA with different PEG lengths. As expected, increasing the hydrophobic PLGA block resulted in a lower gelling temperature because the system required less energy to overcome the hydrogen bonding between hydrophilic PEG segments via PLGA-PLGA hydrophobic interactions. A linear association between declining PLGA block length and gelling temperature was discovered [40]. Table 15.2 represents a summary of the factors affecting the characteristics of the copolymeric micelles composed of PLGA-PEG-PLGA.

Table 15.2 Parameters affecting formation and characteristics of PLGA-PEG-PLGA copolymeric micelles

Parameter	Finding	Reference
MWD of PEG block	Larger micelles and looser micelle coronae emerged from a wider dispersion of PEG block	[35]
LA and GA sequence in the PLGA block	Gelling and micellization behaviour were shown to be controllable by modifying the sequence structure in the PLGA block	[24]
Length of PEG block	Short PEG block produce asymmetric (ellipsoid) forms in dilute solution, and a longer PEG block may be characterised using a spherical core-shell model	[37]
LA/GA ratio	A polydisperse system was favoured by the low LA-to-GA ratio, and a monodisperse system was seen with a high LA-to-GA ratio	[38]
PEG/PLGA ratio	Increasing the hydrophobic PLGA block resulted in a lower gelling temperature	[40]

5 Pharmacokinetics (PK) and Pharmacodynamics (PD) of Copolymeric Micelles Based on PLGA-PEG-PLGA

The link between pharmacokinetics and pharmacodynamics is an essential component in the pharmaceutical industry's discovery and development of novel medications. Scientists can use effective PK/PD study design, analysis, and interpretation to better comprehend the correlation between PK and PD, as well as discover PK features for further improvement and optimal drug design and development [41]. PK-PD modelling has been extensively employed to increase insight of the in vivo behaviour of these complicated delivery systems and aid their development since it allows for the separation of drug-, carrier-, and pharmacological system-specific factors [42]. It connects the concentration-time profile measured by pharmacokinetics to the magnitude of the observed reaction measured by pharmacodynamics [43].

Localized cancer therapies involving a mixture of medications have lately surfaced as novel strategies for preventing tumour progression and recurrence. Ma et al. designed a new method for treating osteosarcoma by employing thermosensitive PLGA-PEG-PLGA hydrogels to offer targeted delivery of more than a single medication, which included doxorubicin (DOX), cisplatin (CDDP), and methotrexate (MTX). In a nude mouse model containing human osteosarcoma Saos-2 xenografts, the drug-loaded hydrogels' anticancer efficacies were assessed *in vivo*. Within the neighbourhood of the tumours, the mice were administered a single injection of drug-loaded hydrogels or solutions of the free drug. Treatment with drug-loaded hydrogels exhibited improved *in vivo* tumour inhibition efficacies for up to 16 days in comparison to treatment with the free drug. The reason for this is likely due to the hydrogels' long-term drug release characteristics, which result in sustained tumour suppression *in vivo* [44].

In another study, Jiang and co-workers used multifunctional dendritic nanoparticles in a thermoresponsive injectable hydrogel matrix made of PLGA-PEG-PLGA to create a localised drug delivery vehicle so as to combine chemotherapy and immunotherapy. PLGA-PEG-PLGA allows for targeted, long-lasting drug administration as well as co-loading of medicinal substances for combination therapy. The dendritic nanoparticles were created with a fourth-generation L-arginine-rich dendritic architecture (G4-Arg) and a hydrophobic interior that could hold the anticancer medication DOX. The 4 T1 murine breast cancer model established from BALB/C mice was used to assess the anticancer impact of the various formulations *in vivo*. After a 24-day therapy, the Gel/G4-Arg/DOX group had the strongest tumour growth suppression efficacy of all the groups. The results also revealed that the tumour volume of the doxorubicin-loaded *in situ* thermosensitive hydrogel group was less as compared to the free doxorubicin group given intravenously. At the end of the treatment period, the group that received Gel/G4-Arg/DOX only once had a stronger tumour growth suppression than the free DOX group, which received free DOX four

times. *In vivo*, the level of NO in tumour tissue in the G4-Arg groups was considerably greater. The better penetrability of G4-Arg, as well as the synergism of NO created by the L-arginine in G4-Arg, can be attributed to the Gel/G4-Arg/ improved DOX's antitumor efficiency [45].

The idea of PLGA-PEG-PLGA micelles encapsulating US597 was conceived by Chen and co-workers with the goal of establishing a delivery system for prolonged oral cancer therapy. The peak plasma concentration of US597@micelles was recorded to be nearly 4 times greater as compared to free US597. US597@micelles had a 4.2-fold faster peak plasma concentration of US597 as compared to free US597. Thus, the US597@micelles were absorbed more rapidly than free US597 in Sprague-Dawley rats, and the degree of absorption as measured by peak plasma drug concentration was substantially greater. There were also alterations in the pharmacokinetic characteristics for US597@micelles, which revealed substantial modifications. US597@micelles had a two-fold shorter elimination half-time ($t_{1/2}$) than free US597 (8.716 ± 7.003 hours for US597@micelles and 16.433 ± 8.821 hours for US597), indicating that US597 was eliminated from the rat plasma more quickly for US597@micelles than for free US597. Furthermore, the change in AUC_{0-t} from $0.274 \pm 0.265 \mu\text{g}\cdot\text{h}\cdot\text{ml}^{-1}$ for US597 to $0.424 \pm 0.22 \mu\text{g}\cdot\text{h}\cdot\text{ml}^{-1}$ for US597@micelles (1.54-fold) suggested that US597@micelles would have better bioavailability as compared to the free drug. Collectively, this evidence suggests that the US597@micelles had better absorption, metabolism, and excretion than free US597, as well as a longer drug action time thereby having a higher solubility and anti-tumour efficacy [46].

In order to co-deliver DOX and β -cyclodextrin curcumin (CD CUR) to tumour regions, Yang and co-workers utilised a hydrogel composed of PLGA-PEG-PLGA. Using K 7 tumour-bearing mice, the anticancer efficacy of various techniques was assessed *in vivo*. Although the group treated with free DOX showed significant anticancer effects, the gel+DOX group had a smaller tumour volume than the free DOX group because the former relied on the sustained release of DOX

from hydrogel to keep a reasonably high DOX concentration at tumour locations for a long period. The ability of curcumin (CUR) to down-regulate Bcl 2, added to the effectiveness of the combination therapy of gel+DOX + CD CUR in killing tumour cells as compared to free DOX. As a result, although gel+CD CUR had a weak anticancer effect, the combination therapy based on gel+DOX + CD CUR had a greater antitumor activity over monotherapy. DOX and CD CUR could be delivered to the tumour region simultaneously using this localised dual medication delivery mechanism. Also, the hydrogel functioned as a drug depot, allowing for long-term medication efficacy thereby proving to be a promising method for slowing down tumour growth [47].

In another study conducted by Nagahama et al., a DOX delivery method that was both safe and effective for localised cancer chemotherapy was developed. Self-assembly of PLGA-PEG-PLGA copolymer micelles, clay nanodisks (CNDs), and DOX resulted in a novel biodegradable injectable gel. In vivo investigations employing human xenograft tumours in nude mice were used to investigate the antineoplastic effect of P3k/CND/DOX hybrid gels. When the tumour volume was 300 mm³, a hybrid gel precursor solution of 300 litres (210 g of DOX) was injected directly into the tumour. Treatment with the P3k/CND/DOX hybrid gel, the tumour volume decreased gradually. Most notably, the reduction lasted for a period of 21 days following a single hybrid gel injection, with no signs of dermatitis. Thus, the P3k/CND/DOX hybrid gel's anticancer efficacy was ascertained. The P3k/CND/DOX hybrid gel's prolonged antineoplastic action was related to the gradual release of DOX and improved cellular uptake of the DOX that was released due to the formation of nanostructures made of DOX with P3k/CND hybrid micelles. As a result, it is determined that a DOX-delivery system for focused cancer treatment requires long-term continuous gradual release of DOX devoid of "burst release" could be provided by an injectable P3k/CND/DOX gel [48].

Recently, an injection of a liposome DOX-loaded PLGA-PEG-PLGA-based thermogel was

produced by Cao and co-workers. Further, in orthotopic 4 T1 breast tumour-bearing BALB/c female mice, the anticancer efficacy of DOX-loaded formulations was investigated in vivo. Free DOX, DOX liposomes, DOX gel, and DOX-loaded liposomal gel groups had tumour inhibition rates of 56.2%, 59.7%, 75.9%, and 86.5%, respectively. Tumour volume was substantially less in the DOX gel and DOX-loaded liposomal gel sustained-release groups, implying that the peritumoural injection had higher antitumour effectiveness. DOX-loaded liposomal gel had the lowest tumour volume of all, measuring 269.9 ± 61.7 mm³, showing the greatest tumour suppression [49].

In order to demonstrate the superiority of the prodrug thermogels, in vivo antitumor effectiveness in a female H22 hepatoma-bearing mice model was studied by Zhang et al. The Gel-CAD(*cis*-aconitic anhydride-functionalized DOX) + DTX group as well as the Gel-SAD(succinic anhydride-modified DOX) + DTX group had stronger tumour inhibition efficacy than the DOX+ docetaxel (DTX) group, which was attributed to the DOX-conjugated thermogels' prolonged drug release profile. Owing to the synergism of a DNA intercalator DOX with a microtubule-interfering DTX, the Gel-CAD + DTX group had the most effective tumour inhibition of all the testing circumstances. Thus, an effective combination of a complimentary medication and a tumour microenvironment-labile polymeric prodrug thermogel presented considerable promise for in situ antineoplastic therapy [33].

By employing a fatty acid-modified Gem derivative as a drug and a thermosensitive hydrogel as the carrier, Yang and group were able to develop a long-acting Gem delivery system. The hydrogels were easily made by combining two types of PLGA-PEG-PLGA copolymers in the right proportions. BALB/c mice with 4 T1 mammary tumours were given different therapies to assess the anticancer efficiency of GemC16@Gel alone as well as the synergetic chemoradiotherapy treatment when paired with irradiation. The best tumour growth suppression was achieved with a single injection of GemC16@Gel with

three times of X-ray exposure (GemC16@Gel + X ray). This was related to GemC16's long-term release as well as its long-lasting radiosensitizing action over multiple X-ray exposures [50].

Very recently, the use of collagenase to modify the extracellular matrix with abundant collagen in solid tumours has been shown to improve interstitial transport and antibody antitumor effectiveness. Thus, Pan and co-workers created a PLGA-PEG-PLGA polymer-based thermosensitive hydrogel for peritumoural injection that included a HER2-targeted monoclonal antibody trastuzumab and collagenase (Col/Tra/Gel). HER2-positive BT474 tumour-bearing mice were chosen, in which the Col/Tra/Gel treatment showed the highest reduction of tumour growth. When compared to the other groups, the drug-loaded hydrogel preparations displayed substantial inhibitory action on tumours. Furthermore, throughout the experiments, all groups of mice preserved their usual weight. These findings showed that subcutaneous therapy with Col/Tra/Gel improved trastuzumab antitumor effectiveness [51].

Jin et al. formulated thermosensitive and formation of *in situ* hydrogels comprising of PLGA-PEG-PLGA that could deliver corilagin and low-molecular-weight chitosan (LC) directly to the tumour tissue by intratumour administration while altering the tumour microenvironment to increase drug penetration. Surprisingly, when corilagin/LC/PPP thermosensitive hydrogels (CCPH) were combined along with Abraxane®, the synergistic tumour inhibition impact could reach 61.24% with the best anticancer activity. This could be attributable to tumour stroma remodelling and increased drug accumulation. After injection, the corilagin/LC/PPP solution efficiently transformed into CCPH in the mice's subcutaneous tissues; its concentration steadily declined. Further, it was totally destroyed on the 12th day, thereby confirming its use as well as its *in vivo* biodegradability. The biodegradation properties of CCPH showed that after the therapy was completed, the CCPH which was implanted could be removed without causing any harm to the body. As a result, when used in clinical settings, the treatment was considered to be safe and

also prevents the need for surgical removal after treatment [52].

To improve anticancer activity and bioavailability *in vivo*, andrographolide was encapsulated in a micelle composed of PLGA-PEG-PLGA. The $AUC_{0-\infty}$ was calculated to be 17.167 h g/ml for andrographolide micelles, which was 2.65-fold higher than the 6.463 h g/ml for free andrographolide suspensions, showing that the micelles encapsulating andrographolide have significantly increased bioavailability. Andrographolide micelles also had a substantially greater mean retention duration with a smaller elimination rate constant (K_{el}), indicating that eliminating the drug from the blood may be much slower and that the medication may remain in the body for a prolonged period for greater efficiency. Thus, these findings proved that PLGA-PEG-PLGA-based micelles enhanced the andrographolide pharmacokinetic behaviour *in vivo*, thereby acting as a promising delivery strategy for long-term drug release [53].

Ci and co-workers reported a preparation containing irinotecan along with PLGA-PEG-PLGA. Data obtained from the study revealed an excellent sustained release profile as well as considerable augmentation of the proportion of the active form of the drug by the thermogel. The tumour volume was also found to grow somewhat after irinotecan/thermogel injection, and then reduced dramatically. On day 21, the relative tumour volumes in the irinotecan/thermogel groups were 0.2 and 0.1, respectively, for medication dosages of 45 and 90 mg/kg/w. The final tumour volume was barely 10% of the initial size, showing that the tumour had shrunk dramatically. In conclusion, the prolonged release of irinotecan from the triblock-based thermogel had a remarkable anticancer efficacy in human SW620 colon carcinoma [54].

Corneal neovascularization (CNV) is a leading cause of ocular surface diseases. Subconjunctival delivery of anti-angiogenic drugs inhibits neovascularization by administering anti-angiogenic drugs in a targeted and effective manner. Liu et al. utilized the triblock copolymer of PLGA-PEG-PLGA in order to deliver metformin and levofloxacin hydrochloride

in a sustained manner. By using a mouse model of corneal alkali burn, the *in vivo* efficiency of subconjunctival administration of the metformin (MET) + levofloxacin hydrochloride (LFH)-loaded thermosensitive hydrogel in suppressing CNV was investigated. The MET+LFH-loaded hydrogel significantly prevented the development of CNV as compared to a single injection of MET or LFH loaded thermosensitive hydrogel. The combination of a long-acting MET together with an antibiotic (LFH) produced a synergistic effect. Therefore, subconjunctival injection of MET and LFH utilising PLGA-PEG-PLGA-based thermosensitive hydrogel holds a lot of promise for ocular anti-angiogenic therapy. Thus, co-delivery of MET and LFH may have a better inhibitory effect on CNV growth [55].

In a study conducted by Chan and co-workers, a continuous evaluation for the formation of neovascularization following an alkali-burn was conducted by scoring the degree of corneal opacity, burn stimulus, neovascularization of vessel growth, and inflammatory response of biomarker IL-6 in a rat model in order to determine the efficiency of dexamethasone (DEX)-loaded PLGA-PEG-PLGA thermogel following subconjunctival administration in the treatment of CNV. The mean scores of the negative control groups were substantially greater in comparison to the groups that received the drug solution and the drug-loaded thermogel in the corneal opacity evaluation, suggesting that the DEX which was subconjunctivally injected was effective in lowering corneal opacity of the burn region following an alkali-burn. The iris features were marginally blurred in the group that received the DEX solution but instead was recognisable in the group that was treated with the DEX-loaded thermogel. Similar to the DEX solution treatment group, eyeballs that received an injection of the drug-loaded thermogel had lower scores in the burn stimulus as well as neovascularization after 7 days of treatment [56].

Zhang and co-workers aimed to create an injectable intravitreal implant made of thermogel that would administer DEX to the posterior portion of the eye for a prolonged time period. The thermogel matrix was formulated using various

block ratios of PLGA-PEG-PLGA copolymers, and the micelles created using the copolymer aided in solubilizing the hydrophobic drug in an aqueous media. The vitreous retention period of DEX suspension proved to be very short for the treatment of chronic eye diseases. Fortunately, the thermogel dramatically delayed DEX intravitreal release, with a 28-fold increase in $MRT_{(0-\infty)}$ of DEX as compared to the suspension (from 4.1 h to 115.8 h). Moreover, initially the concentration of DEX given by the thermogel in the vitreous was well-maintained at less than 10 $\mu\text{g}/\text{mL}$ that is nearly twofold lower as compared to the suspension's peak concentration. Thus, this property suggested that, once delivered, the aqueous copolymeric solution quickly converted to a semisolid gel in the physiological milieu of the eye, inhibiting the first burst release considerably [57].

Xie and colleagues developed an injectable thermo-sensitive Avastin®/PLGA-PEG-PLGA hydrogel to determine the feasibility of an intravitreal injection of the PLGA-PEG-PLGA hydrogels. Avastin® was released in the retina of a rat model for at least 6 weeks after intravitreal injection of Avastin®/hydrogel. The C_{max} in the retina of rats that received an injection of the aqueous solution of Avastin® was 38.05 ± 15.56 ng/mg. The data showed that intravitreal injections of Avastin®/PLGA-PEG-PLGA hydrogel might significantly lengthen Avastin® *in vivo* half-life in the vitreous humour and retina. The *in vivo* pharmacokinetic study indicated that the PLGA-PEG-PLGA hydrogel was able to prolong the release of Avastin® in the vitreous humour and retina in comparison to injection of an aqueous solution of Avastin® [58].

Buprenorphine is an extremely lipophilic opioid partial agonist which inhibits the signs and symptoms caused due to withdrawal syndrome. Kamali and co-workers developed a long-acting buprenorphine injectable implant comprising of PLGA-PEG-PLGA and N-methyl-2-pyrrolidone (NMP) that possessed increased therapeutic efficacy. As a result, combining PLGA-PEG-PLGA with NMP proved to be an excellent formulation in order to obtain a long-acting, controlled-release, injectable

buprenorphine solution-delivery system devoid of the initial burst release. Additionally, in comparison to the subcutaneous administration of the solution, the AUC of buprenorphine and Norbuprenorphine was increased when the in situ forming gel and in situ forming implant were used. In contrast to the in situ forming gel and in situ forming implant formulations, a considerable percentage of administered buprenorphine solution in NMP seemed to be unabsorbed and did not enter blood circulation from the site of administration. In addition, the AUC and serum concentration (C) range of buprenorphine with regard to the in situ forming gel ($AUC = 2721.38$ 69, $C = 1.87$ – 7.12) preparation were almost the same as the in situ forming implant (RBP-6000) ($AUC = 2727.36$ 71, $C = 1.75$ – 10), thereby suggesting that the in situ forming gel could achieve the required therapeutic concentration required to treat opioid and alcohol addiction [59].

Bacterial infection is a major stumbling block in the treatment of wounds, as it promotes the development of exudate and slows the healing cycle. In order to distribute teicoplanin, which is a glycopeptide antibiotic that is employed for cutaneous wound healing, Xu and co-workers developed a thermogelling dressing system consisting of two triblock copolymers of PLGA-PEG-PLGA featuring varying block lengths. At room temperature, the teicoplanin-loaded thermogel was observed to be a free-flowing sol that solidified into a semi-solid gel at physiological temperature. In order to test the efficiency of the teicoplanin-loaded thermogel formulation, a full-thickness excision wound model in Sprague-Dawley rats was created. The thermogel was found to reduce the inflammatory response, improve the collagen disposition, boost angiogenesis, as well as hasten the closure of the wound and healing in Sprague-Dawley rats, according to gross and histopathologic data. The increased wound healing activity was due to the union of teicoplanin's bioactivity and the acidic composition of the thermogel matrix. The application of the thermogel suppressed inflammatory response, expedited re-epithelization, enhanced collagen production and disposition, and stimulated angiogenesis in in vivo experiments, conse-

quently improving wound healing. As a result, the teicoplanin-incorporated PLGA-PEG-PLGA thermogel is a viable option for full-thickness excision wound healing as a wound dressing [60].

El-Zaafarany and co-workers investigated a duo of thermo-responsive hydrogels and emulsomes which were lipid-based in drug transportation from the nose to the brain. In comparison to simple solutions, the application of nanocarriers for direct delivery from the nose to the brain offers immense potential for increasing brain drug levels. The antiepileptic medication oxcarbazepine was encapsulated in emulsomes and further incorporated into a thermogel made of PLGA-PEG-PLGA. The intranasal emulsomal thermogel instillation at a T_{max} of 120 minutes yielded the greatest C_{max} of 3818.8 ng/mL ($p < 0.01$), which was followed by Trileptal® suspension and intranasally administered emulsomes, which yielded C_{max} values of 2567.6 and 2514.4 ng/mL at T_{max} values of 45 and 120 minutes, respectively, and ultimately the intranasally administered oxcarbazepine solution yielded the least. The greatest $AUC_{0-2880min}$ was obtained ($p < 0.05$) in the following order: intranasal thermogel, intranasal oxcarbazepine emulsomes, Trileptal® suspension, and intranasal oxcarbazepine solution. Moreover, the MRT in plasma for emulsomes and thermogel preparations was 58.7- and 76.5-fold higher as compared to the intranasal oxcarbazepine solution, respectively. The plasma half-life of the thermogel was reported to be 1.2-fold higher than that of the oxcarbazepine emulsomes, and significantly greater than the OX solution and Trileptal® suspension, at 6.4 and 5.3 times, respectively ($p < 0.05$). The lipophilic character of the emulsomes may facilitate the partitioning of the drug present in the emulsomes into the cell membrane of the nasal epithelium and deeper into the systemic circulation, thereby explaining the lengthy plasma residency of oxcarbazepine when supplied in conjunction with emulsomes. The emulsomal thermogel's substantial absorption of oxcarbazepine, as seen by the $AUC_{0-2880min}$ and lengthy mean residence time in comparison to intranasal oxcarbazepine-solution, could be due

in part to the gel formulation's high viscosity, which increased the time of contact with the nasal mucosa, boosting the penetrability of oxcarbazepine-emulsomes and/or free oxcarbazepine via the nasal mucosa into the systemic circulation. In comparison to the free drug, the pharmacokinetic data showed that the emulsomes encapsulating oxcarbazepine reduced the rate of its elimination, maintained a high amount of the drug in the circulation, together with a greater circulatory time in the animals [61].

Similarly, nasal oxcarbazepine-emulsome delivery led to the greatest C_{\max} of oxcarbazepine in the brain, which was about 3.3-, 22.9-, and 4.8-fold greater as compared to the emulsome-loaded thermogel, intranasal solution, and the marketed preparation of Trileptal® suspension, respectively. On the contrary, the oxcarbazepine-emulsome-loaded thermogel exhibited greater mean residence durations in the brain than the oxcarbazepine-emulsomes, intranasal oxcarbazepine solution, and Trileptal® suspension. Furthermore, oxcarbazepine was found in the brain even 48 hours after intranasal administration of the emulsomal thermogel, potentially resulting in greater seizure control in patients for an extended duration. Despite the fact that intranasal administration of emulsomal thermogel resulted in a reduced C_{\max} in the brain, the MRT data was higher. When opposed to antiepileptic drug therapies that release the medicines quickly, formulations with prolonged brain residence allow for a longer dosage interval, which not only improves compliance by the patient but also reduces the chances of a seizure occurrence following a missed dose. Likewise, prolonged oxcarbazepine formulations were found to have superior tolerability and greater maintenance dosages than rapid action formulations in treating focal epilepsy [61].

Albendazole, a commonly used anthelmintic, is thought to be effective against helminths because of its major metabolite, albendazole sulfoxide. Feng and group effectively synthesised an albendazole sulfoxide-loaded thermo-sensitive hydrogel. When compared to plain albendazole sulfoxide, *in vivo* pharmacokinetics data suggested that albendazole sulfoxide-loaded hydro-

gel was a more preferable candidate for sustained release. An intraperitoneal injection of albendazole sulfoxide solution (30 mg/kg) resulted in a maximal concentration of (131.98 ng/ml) after 2 hours and then a progressive drop over 72 hours, whereas intraperitoneal administration of albendazole sulfoxide-loaded hydrogel resulted in a maximum concentration of 178.09 ng/ml after 120 hours after which there was a steady reduction. Meanwhile, the albendazole sulfoxide-loaded hydrogel had a longer mean residence time ($MRT_{0-\infty}$) (66.892 h) than the albendazole sulfoxide solution (46.931) [62].

Tissue expanders are useful tools for creating additional skin for reconstructive surgery. The use of hydrogel tissue expanders eliminates the need for fluid injections on a regular basis. If there is not an exterior membrane, the cross-linked network of hydrophilic polymer allows for intrinsically regulated swelling. A rat skin animal model was used by Garner et al. to characterise these novel hydrogel expanders *in vivo*. The amount of hydrophobic polyester in the hydrogel was found to minimise swelling velocity to a rate and volume that eliminated the risk of the premature swelling from rupture of the sutured region. Furthermore, enhancing the cross-linking density gave the hydrogel considerable mechanical resilience to permit full post-swelling clearance without breaking or crumbling. Also, the addition of more hydrophobic PLGA is expected to impede the breakdown of the cross-linker, resulting in persistent swelling [63].

The encapsulation of propranolol-loaded liposomes in microspheres constructed with PLGA-PEG-PLGA copolymer was suggested by Guo and group, for topical application so as to achieve prolonged release of the drug in order to lessen the undesirable effects as well as the frequent administration of propranolol in the treatment of infantile hemangioma. Tumour inhibition of subcutaneous infantile hemangioma in nude mice was investigated. The therapy led to an 84% reduction in the volume of the hemangioma by day 35, but the liposomes and propranolol therapy only led in a 44% and 13% reduction in the volume of the hemangioma, respectively. In comparison to the starting hemangioma volume of

25 mm³, the volume of the hemangioma had risen 7.2 times and 4.8 times in the mice that were administered propranolol and in the mice that received the propranolol liposomes, respectively. The gradual decline in the release of propranolol from the microspheres could ultimately produce a lower cytotoxic impact. The extended and continuous release of propranolol from the microspheres, on the other hand, would dramatically slow hemangioma angiogenesis [64].

Li and co-workers synthesised a thermoresponsive PLGA-PEG-PLGA copolymer, and further the safety and efficiency of the PLGA-PEG-PLGA thermogel in preventing peridural fibrosis in an adult rat laminectomy model was assessed. Anatomical inspections and histological investigations were conducted after 30 days following the surgical procedure to assess the thermogel's efficacy in the prevention of epidural fibrosis. Clinical observation revealed that the freedom of nerve roots was unaffected by the expansion of the thermogel during the gelling process, implying that the swelling was minor and the thermogel was sufficiently soft to avoid compression [65].

Huang and co-workers used a rat model of brachial plexus avulsion to determine the therapeutic efficacy of a quercetin incorporated PLGA-PEG-PLGA based hydrogel. Results of the study indicated that the hydrogel with a higher amount of quercetin may be more effective at reducing oxidative stress and inflammation in secondary injury, as well as protecting nerve tissues in the initial phases of nerve damage. The quercetin-loaded hydrogel sustained-release technology was thought to act by suppressing the neuronal autophagy and death through activation of the PI3K/Akt pathway and inhibition of the ERK1/2 pathway, together with lowering oxidative stress and inflammation. An increased number of motor neurons present in the damaged spinal cord were preserved following treatment with hydrogels possessing varying concentrations of quercetin, thereby laying a foundation for further nerve healing. Thus, the results indicate that the quercetin-loaded copolymeric gel had the ability to increase axon intrinsic growth as well as improve peripheral nerve function recovery [66].

For reducing the first burst release, an in situ forming composite of naltrexone was developed by Kamali and co-workers, by utilising PLGA-PEG-PLGA and N-methyl-2-pyrrolidone. The developed formulation (in situ forming composite) was able to reduce the first burst release, according to the C_{\max} data. In addition, the AUC, absolute bioavailability, and range of serum naltrexone concentrations for the in situ forming composite were similar to those for Vivitrol®. The in situ forming composite system was thus found to be biocompatible and an effective formulation for naltrexone continuous release with low initial burst release [67].

Recently Rong et al. produced a delivery system for insulin by incorporating chitosan nanoparticles into a PLGA-PEG-PLGA hydrogel. Subconjunctival administration of the hydrogel decreased the decline in scotopic B-wave amplitude, relieved micro- and ultrastructural abnormalities in the retina, and decreased apoptosis of the retinal cell in diabetic retinopathy rats as compared to the other groups. However, in the ICNPH group, there was a significant decrease in vascular endothelial growth factor as well as glial fibrillary acidic protein expression, together with a substantial rise in the expression of occludin, in comparison to the sham treatment group. These findings proved that subconjunctival injection of ICNPH had a considerable neuroprotective impact on retinas in diabetic retinopathy rats and promoted regulated insulin delivery [68].

A series of PCLA-PEG-PCLA and PLGA-PEG-PLGA mixed hydrogels were produced and studied by Wang et al. A mixed hydrogel was also chosen for the preparation of the Depot-gel-in-Ms-in-Matrix-gel system for the treatment of type 2 diabetes mellitus. PLGA microspheres (Ms) were used to encapsulate exenatide-loaded hydrogels, which were then enclosed in blank hydrogel. Injecting the above prepared formulation resulted in a stable blood glucose concentration in the treated mice as well as well-maintained body weight for a period of 20 days in the pharmacodynamics investigation. The effects of Ms. and Depot-gel-in-Ms-in-Matrix-gel were compared using OGTT on the 20th day after the injection. The blood glucose fluctuations of both

the Depot-gel-in-Ms-in-Matrix-gel and the exenatide solution groups were reduced. The Ms. group, on the other hand, experienced just as much variation as the blank medium solution group. These findings revealed that in the Depot-gel-in-Ms-in-Matrix-gel group, high bioactive exenatide release was maintained, whereas in the Ms. group, it was terminated. Thus, the Depot-gel-in-Ms-in-Matrix-gel was found to be a potential exenatide-loaded long-acting preparation for treating diabetes [69].

Wang and group created a kartogenin-loaded thermoresponsive gel for intra-articular administration in order to bring forth such a carrier for prolonged release of cartilage-protective agent for the possible use of osteoarthritis (OA) treatment. As a kartogenin carrier for intra-articular injection, a PLGA-PEG-PLGA thermogel was formulated. A rabbit OA model was used to determine the *in vivo* effect of the kartogenin thermogel. A knee OA model utilising the ACLT technique was developed to confirm the possibility of employing kartogenin thermogel to treat OA. Histological staining, OARSI score, and synovial fluid measurement of inflammatory cytokines revealed that OA knees that received treatment with kartogenin thermogel had considerably higher cartilage regeneration and decreased inflammatory joints. The *in vivo* findings strongly suggested that kartogenin has anti-arthritis and chondroprotective properties for the treatment of arthritis [70].

In another study, Yan and group synthesised PLGA-PEG-PLGA loaded with simvastatin. A rat bone defect model was also used to illustrate the properties of this composite *in vivo*. In comparison to samples treated with PLGA-PEG-PLGA and control samples, bone deformities injected with simvastatin/PLGA-PEG-PLGA hydrogel demonstrated higher new bone growth. Therefore, this study's findings showed that simvastatin/PLGA-PEG-PLGA may have therapeutic prospective for bone repair [71].

In the work carried out by Liu et al., PLGA-PEG-PLGA solution was combined with a compound of salmon calcitonin (sCT) and oxidised calcium alginate (OCA) in this work. This preparation was then administered to female Sprague-

Dawley rats suffering from osteopenia to create a hydrogel that would provide long-term treatment. The polymer formulation groups received sCT therapy, which resulted in a near-complete repair of the bone structure physiologically as well as biomechanical qualities in the rat femora of Sprague-Dawley due to the sustained and consistent release of sCT. As a result of the prolonged and consistent release of sCT, the capacity for deformation of the bone was dramatically increased. Hydrogels that released sCT partially repaired the femora of MPA-induced osteopenic Sprague-Dawley rats. As a result, the formulated hydrogel containing the incorporated sCT-OCA complex showed a lot of promise for long-term osteopenia treatment [72].

Recently Xu and co-workers created a thermoresponsive PLGA-PEG-PLGA-based hydrogel supported by upconversion hollow microtubes (UCHMs) with great mechanical properties together with a strong upconversion luminescence to monitor noninvasive bone regeneration. The monitoring of the bone deformities mending procedure was realised, which included the degradation of composite hydrogel scaffold material as well as regeneration of the bone in the defect location, owing to the upconversion luminous feature of the composite hydrogel. After 4 weeks, the composite hydrogel scaffolds were entirely destroyed, and following 6 weeks of bone regeneration, the defect site was totally healed. Thus, the hydrogel provides considerable promise during the clinical therapy of bone defects based on bone healing efficiency, real-time monitoring capability, and biological safety [73].

Kartogenin (KGN), a new chondroinductive non-protein small molecule, was introduced in a thermogel composed of PLGA-PEG-PLGA in order to produce a microenvironment of bone marrow mesenchymal stem cells for the regeneration of cartilage. The group which administered the aforementioned formulation had the most cartilage regeneration, and the flaw was completely healed after a period of 3 months. Even after 8 weeks, the group which administered the thermogel was found to have the best ICRS macroscopic score values. The implantation of the thermogel revealed the best histological

repair of the cartilage, most efficient ECM deposition, and greatest mechanical strength, indicating one of the most successful in-vivo cartilage regeneration [74].

Zheng and colleagues created a thermosensitive PLGA-PEG-PLGA-based injectable hydrogel containing baricitinib (Bari-P hydrogel). In vivo results revealed that Bari-P hydrogel therapy inhibits JAK2, STAT3 phosphorylation, suppresses inflammatory cytokine production, and lowers neuronal death. Bari-P hydrogel also prevented neuronal death during the early stages of damage as well as promoted enhanced functional recovery during later stages, according to histopathological and behavioural testing. Therefore, by blocking the JAK2-STAT3 pathway and limiting the expression of inflammatory cytokines during the early phases of damage, Bari-P hydrogel decreased neuronal death and enhanced functional recovery in spinal cord damaged rats [75].

Animal contraception and control of fertility are in high demand in the livestock and pet industries. To achieve long-acting animal contraception, Chen et al. proposed a preparation comprising of an injectable and biodegradable thermogel for the sustained delivery of a hormonal contraceptive, i.e. levonorgestrel. The PLGA-PEG-PLGA micelles generated in water by amphiphilic polymer carriers could act as a repository for hydrophobic levonorgestrel molecules to be dissolved. The utilization of PLGA-PEG-PLGA thermogel increased the release of levonorgestrel following subcutaneous injection in SD rats, according to in vivo pharmacokinetic experiments. As a result, this research found that, injecting a PLGA-PEG-PLGA thermogel was a possible contender for long-term levonorgestrel release, and that it offered an appealing choice for long-term animal contraception and reproductive control due to its ease of fabrication, ease of administration, and low cost. To assess in vivo pharmacokinetics, two levonorgestrel-loaded gel formulations with the same drug dosage (2.5 mg/mL, 0.6 mL and 5 mg/mL, 0.3 mL) were subcutaneously administered into SD rats. The two gel formulations both had a minor initial burst. The C_{\max} of 7.20 ± 0.93 ng/mL was reached in the first

4 hours after injection of the 2.5 mg/mL levonorgestrel-loaded gel formulation, and the C_{\max} of 6.40 ± 1.07 ng/mL was similarly achieved in the first 4 hours following injection of the 5 mg/mL LNG-loaded thermogel system. Following that, for 2.5 and 5 mg/mL levonorgestrel-loaded thermogel systems, respectively, the drug plasma concentration remained stable above the minimal effective plasma concentration of levonorgestrel (0.2 ng/mL) for 2 and 3 weeks, demonstrating that a single administration of levonorgestrel-loaded gel formulation might exert a sustained contraceptive action for several weeks. Although the two gel formulations including levonorgestrel had identical bioavailability due to the same drug dosage, the 2.5 mg/mL levonorgestrel-loaded thermogel had a shorter mean residence time ($MRT_{0.1}$) than the 5 mg/mL gel formulation. The in vivo data was very similar to the in vitro release profiles, with the extended release period due to increased drug loading quantities. The levonorgestrel-loaded PLGA-PEG-PLGA thermogel system appears to be one of the most promising animal contraception solutions in the future, especially given the low cost of raw materials and ease of manufacture and administration [76]. Table 15.3 enlists few of the applications of the copolymeric micelles comprising of PLGA-PEG-PLGA in drug delivery.

6 Conclusion

The application of thermo-responsive copolymers has grown in popularity since the past couple of years, notably in the sector of controlled release. In drug delivery research, they are arguably one of most investigated class of environment-sensitive polymers. At a given temperature, these hydrogels can quickly transform from a low viscosity fluid into a highly viscous gel. The triblock copolymers possess thermo-responsive features wherein the solution state of these polymers undergo conversion to a highly viscous gel form at body temperature. Due to their biodegradability and since they have a high safety profile, PLGA-PEG-PLGA triblock copo-

Table 15.3 Applications PLGA-PEG-PLGA copolymeric micelles in drug delivery

Therapeutic cargo	Disease Condition	Drug delivery system	References
Combretastatin	Cancer	Nano-micelles	[77]
Doxorubicin	Osteosarcoma	Hydrogel scaffold	[78]
Bovine serum albumin		Hydrogel	[79]
Brimonidine	Glaucoma	Layered double hydroxide (LDH) nanoparticle/thermogel	[80]
Amphotericin B	Cryptococcal meningitis	Thermogel	[81]
Voriconazole	Keratomycosis	Thermogel	[82]
Berberine	Hypercholesterolemia	Nanoparticles	[83]
Bupivacaine	Peripheral nerve blockade	Hydrogels	[84]

lymers are appealing materials. Simple compounding, filtration sterilisation, and the usage of water as a solvent are just a few of the benefits. Although these triblock copolymers are excellent prospects for further investigation in the field of medication delivery, there is still a significant need for additional studies before it can be employed in the clinical setting.

Acknowledgments The authors are thankful to MAHE for providing fellowship to Miss. Shirleen Miriam Marques. The authors acknowledge the support of Manipal College of Pharmaceutical Sciences, Manipal Academy of Higher Education, Manipal, Karnataka, India, for providing infrastructural facilities.

Conflict of Interest The authors report no conflicts of interest in this work.

References

- Song Z, Feng R, Sun M, et al. Curcumin-loaded PLGA-PEG-PLGA triblock copolymeric micelles: preparation, pharmacokinetics and distribution in vivo. *J Colloid Interface Sci.* 2011;354(1):116–23.
- Hirani A, Grover A, Lee YW, et al. Triamcinolone acetate nanoparticles incorporated in thermoreversible gels for age-related macular degeneration. *Pharm Dev Technol.* 2016;21(1):61–7.
- Zheng L, Wang L, Qin J, et al. New biodegradable implant material containing hydrogel with growth factors of lyophilized PRF in combination with an nHA/PLGA scaffold. *J Hard Tissue Biol.* 2015;24(1):54–60.
- Babos G, Biró E, Meiczinger M, Feczko T. Dual drug delivery of sorafenib and doxorubicin from PLGA and PEG-PLGA polymeric nanoparticles. *Polymer.* 2018;10(8):895.
- Wilkosz N, Łazarski G, Kovacik L, et al. Molecular insight into drug-loading capacity of PEG-PLGA nanoparticles for itraconazole. *J Phys Chem B.* 2018;122(28):7080–90.
- Yen Y, Yu L, Qian H, et al. In vivo evaluation of cisplatin-loaded PEG-PCL block copolymeric nanoparticles for anticancer drug delivery. *Ann Oncol.* 2019;30:v191.
- Balci B, Top A. PEG and PEG-peptide based doxorubicin delivery systems containing hydrazone bond. *J Polym Res.* 2018;25(4):1–12.
- Crowley ST, Poliskey JA, Baumhover NJ, Rice KG. Efficient expression of stabilized mRNA PEG-peptide polyplexes in liver. *Gene Ther.* 2015;22(12):993–9.
- Zhou N, Zhi Z, Liu D, et al. Acid-responsive and biologically degradable polyphosphazene nanodrugs for efficient drug delivery. *ACS Biomater Sci Eng.* 2020;6(7):4285–93.
- Hou S, Chen S, Dong Y, Gao S, Zhu B, Lu Q. Biodegradable cyclomatrix polyphosphazene nanoparticles: a novel pH-responsive drug self-framed delivery system. *ACS Appl Mater Interfaces.* 2018;10(31):25983–93.
- Yu L, Zhang Z, Zhang H, Ding J. Mixing a sol and a precipitate of block copolymers with different block ratios leads to an injectable hydrogel. *Biomacromolecules.* 2009;10(6):1547–53.
- Khaledi S, Jafari S, Hamidi S, Molavi O, Davaran S. Preparation and characterization of PLGA-PEG-PLGA polymeric nanoparticles for co-delivery of 5-fluorouracil and Chrysin. *J Biomater Sci Polym Ed.* 2020;31(9):1107–26.
- Zahoranova A, Vojtova L, Dusicka E, Michlovska L, Krivankova N, Baudis S. Hybrid hydrogel networks by photocrosslinking of thermoresponsive α , ω -Itaconyl-PLGA-PEG-PLGA micelles in water: influence of the lithium Phenyl-2, 4, 6-Trimethylbenzoylphosphinate photoinitiator. *Macromol Chem Phys.* 2020;221(17):2000165.
- Jeong B, Bae YH, Kim SW. Biodegradable thermosensitive micelles of PEG-PLGA-PEG tri-

- block copolymers. *Colloids Surf B: Biointerfaces*. 1999;16(1-4):185–93.
15. Makadia HK, Siegel SJ. Poly lactic-co-glycolic acid (PLGA) as biodegradable controlled drug delivery carrier. *Polymers*. 2011;3(3):1377–97.
 16. Wang X, Zhang Y, Xue W, Wang H, Qiu X, Liu Z. Thermo-sensitive hydrogel PLGA-PEG-PLGA as a vaccine delivery system for intramuscular immunization. *J Biomater Appl*. 2017;31(6):923–32.
 17. Wang SJ, Zhang ZZ, Jiang D, et al. Thermogel-coated poly (ϵ -caprolactone) composite scaffold for enhanced cartilage tissue engineering. *Polymers*. 2016;8(5):200.
 18. Chen Y, Shi J, Zhang Y, et al. An injectable thermo-sensitive hydrogel loaded with an ancient natural drug colchicine for myocardial repair after infarction. *J Mater Chem B*. 2020;8(5):980–92.
 19. Wang M, Zhan J, Xu L, et al. Synthesis and characterization of PLGA-PEG-PLGA based thermosensitive polyurethane micelles for potential drug delivery. *J Biomater Sci Polym Ed*. 2020;32:613–34.
 20. Zentner GM, Rath R, Shih C, et al. Biodegradable block copolymers for delivery of proteins and water-insoluble drugs. *J Control Release*. 2001;72(1-3):203–15.
 21. Ghahremankhani AA, Dorkoosh F, Dinarvand R. PLGA-PEG-PLGA tri-block copolymers as an in-situ gel forming system for calcitonin delivery. *Polym Bull*. 2007;59(5):637–46.
 22. Michlovská L, Vojtová L, Mravcová L, Hermanová S, Kučerík J, Jančář J. Functionalization conditions of PLGA-PEG-PLGA copolymer with Itaconic anhydride. *Macromol Symp*. 2010;295(1):119–27.
 23. Qiao M, Chen D, Ma X, Liu Y. Injectable biodegradable temperature-responsive PLGA-PEG-PLGA copolymers: synthesis and effect of copolymer composition on the drug release from the copolymer-based hydrogels. *Int J Pharm*. 2005;294(1-2):103–12.
 24. Yu L, Zhang Z, Ding J. Influence of LA and GA sequence in the PLGA block on the properties of thermogelling PLGA-PEG-PLGA block copolymers. *Biomacromolecules*. 2011;12(4):1290–7.
 25. Kitayama T, Hatada K. *NMR spectroscopy of polymers*. Dordrecht, Holland: Springer Science & Business Media; 2013.
 26. Ghahremankhani AA, Dorkoosh F, Dinarvand R. PLGA-PEG-PLGA tri-block copolymers as in situ gel-forming peptide delivery system: effect of formulation properties on peptide release. *Pharm Dev Technol*. 2008;13(1):49–55.
 27. Khodaverdi E, Tekie FSM, Mohajeri SA, Ganji F, Zohuri G, Hadizadeh F. Preparation and investigation of sustained drug delivery systems using an injectable, thermosensitive, in situ forming hydrogel composed of PLGA-PEG-PLGA. *AAPS PharmSciTech*. 2012;13(2):590–600.
 28. Chen S, Pieper R, Webster DC, Singh J. Triblock copolymers: synthesis, characterization, and delivery of a model protein. *Int J Pharm*. 2005;288(2):207–18.
 29. Kowalczyk D, Pitucha M. Application of FTIR method for the assessment of immobilization of active substances in the matrix of biomedical materials. *Materials*. 2019;12(18):2972.
 30. Mohajeri SA, Yaghoubi S, Abdollahi E, et al. In-vivo study of naltrexone hydrochloride release from an in-situ forming PLGA-PEG-PLGA system in the rabbit. *J Drug Deliv Sci Technol*. 2016;36:156–60.
 31. Vojtova L, Michlovska L, Valova K, et al. The effect of the thermosensitive biodegradable PLGA-PEG-PLGA copolymer on the rheological, structural and mechanical properties of thixotropic self-hardening tricalcium phosphate cement. *Int J Mol Sci*. 2019;20(2):391.
 32. Mohammadpour F, Kamali H, Hadizadeh F, et al. The PLGA microspheres synthesized by a thermosensitive hydrogel emulsifier for sustained release of risperidone. *J Pharm Innov*. 2021:1–13.
 33. Zhang Y, Zhang J, Xu W, Xiao G, Ding J, Chen X. Tumor microenvironment-labile polymer–doxorubicin conjugate thermogel combined with docetaxel for in situ synergistic chemotherapy of hepatoma. *Acta Biomater*. 2018;77:63–73.
 34. Nasrollahi P, Khajeh K, Tamjid E, Taleb M, Soleimani M, Nie G. Sustained release of sodium deoxycholate from PLGA-PEG-PLGA thermosensitive polymer. *Artif Cells Nanomed Biotechnol*. 2018;46(sup2):1170–7.
 35. Chen L, Ci T, Yu L, Ding J. Effects of molecular weight and its distribution of PEG block on micellization and thermogellability of PLGA-PEG-PLGA copolymer aqueous solutions. *Macromolecules*. 2015;48(11):3662–71.
 36. Chen L, Ci T, Li T, Yu L, Ding J. Effects of molecular weight distribution of amphiphilic block copolymers on their solubility, micellization, and temperature-induced sol–gel transition in water. *Macromolecules*. 2014;47(17):5895–903.
 37. Khorshid NK, Zhu K, Knudsen KD, Bekhradnia S, Sande SA, Nyström B. Novel structural changes during temperature-induced self-assembling and gelation of PLGA-PEG-PLGA triblock copolymer in aqueous solutions. *Macromol Biosci*. 2016;16(12):1838–52.
 38. Sulaiman TNS, Larasati D, Nugroho AK, Choiri S. Assessment of the effect of PLGA co-polymers and PEG on the formation and characteristics of PLGA-PEG-PLGA co-block polymer using statistical approach. *Adv Pharm Bull*. 2019;9(3):382.
 39. Cespi M, Bonacucina G, Tiboni M, Casettari L, Cambriani A, Fini F, Perinelli DR, Palmieri GF. Insights in the rheological properties of PLGA-PEG-PLGA aqueous dispersions: Structural properties and temperature-dependent behaviour. *Polymer*. 2021;213:123216.
 40. Steinman NY, Haim-Zada M, Goldstein IA, et al. Effect of PLGA block molecular weight on gelling temperature of PLGA-PEG-PLGA thermoresponsive copolymers. *J Polym Sci A Polym Chem*. 2019;57(1):35–9.

41. Tuntland T, Ethell B, Kosaka T, et al. Implementation of pharmacokinetic and pharmacodynamic strategies in early research phases of drug discovery and development at Novartis Institute of Biomedical Research. *Front Pharmacol.* 2014;5:174.
42. Zou H, Banerjee P, Leung SSY, Yan X. Application of pharmacokinetic-pharmacodynamic modeling in drug delivery: development and challenges. *Front Pharmacol.* 2020;11:997.
43. Derendorf H, Lesko LJ, Chaikin P, et al. Pharmacokinetic/pharmacodynamic modeling in drug research and development. *J Clin Pharmacol.* 2000;40(12):1399–418.
44. Ma H, He C, Cheng Y, et al. Localized co-delivery of doxorubicin, cisplatin, and methotrexate by thermosensitive hydrogels for enhanced osteosarcoma treatment. *ACS Appl Mater Interfaces.* 2015;7(49):27040–8.
45. Jiang L, Ding Y, Xue X, et al. Entrapping multifunctional dendritic nanoparticles into a hydrogel for local therapeutic delivery and synergetic immunochemotherapy. *Nano Res.* 2018;11(11):6062–73.
46. Chen X, Chen J, Li B, et al. PLGA-PEG-PLGA triblock copolymeric micelles as oral drug delivery system: in vitro drug release and in vivo pharmacokinetics assessment. *J Colloid Interface Sci.* 2017;490:542–52.
47. Yang Z, Liu J, Lu Y. Doxorubicin and CD-CUR inclusion complex co-loaded in thermosensitive hydrogel PLGA-PEG-PLGA localized administration for osteosarcoma. *Int J Oncol.* 2020;57(2):433–44.
48. Nagahama K, Kawano D, Oyama N, Takemoto A, Kumano T, Kawakami J. Self-assembling polymer micelle/clay nanodisk/doxorubicin hybrid injectable gels for safe and efficient focal treatment of cancer. *Biomacromolecules.* 2015;16(3):880–9.
49. Cao D, Zhang X, Akabar M, et al. Liposomal doxorubicin loaded PLGA-PEG-PLGA based thermogel for sustained local drug delivery for the treatment of breast cancer. *Artif Cells Nanomed Biotechnol.* 2019;47(1):181–91.
50. Yang X, Chen X, Wang Y, Xu G, Yu L, Ding J. Sustained release of lipophilic gemcitabine from an injectable polymeric hydrogel for synergistically enhancing tumor chemoradiotherapy. *Chem Eng J.* 2020;396:125320.
51. Pan A, Wang Z, Chen B, et al. Localized co-delivery of collagenase and trastuzumab by thermosensitive hydrogels for enhanced antitumor efficacy in human breast xenograft. *Drug Deliv.* 2018;25(1):1495–503.
52. Jin X, Fu Q, Gu Z, Zhang Z, Lv H. Injectable coriagin/low molecular weight chitosan/PLGA-PEG-PLGA thermosensitive hydrogels for localized cancer therapy and promoting drug infiltration by modulation of tumor microenvironment. *Int J Pharm.* 2020;589:119772.
53. Zhang J, Li Y, Gao W, Repka MA, Wang Y, Chen M. Andrographolide-loaded PLGA-PEG-PLGA micelles to improve its bioavailability and anticancer efficacy. *Expert Opin Drug Deliv.* 2014;11(9):1367–80.
54. Ci T, Chen L, Yu L, Ding J. Tumor regression achieved by encapsulating a moderately soluble drug into a polymeric thermogel. *Sci Rep.* 2014;4(1):1–13.
55. Liu D, Wu Q, Zhu Y, et al. Co-delivery of metformin and levofloxacin hydrochloride using biodegradable thermosensitive hydrogel for the treatment of corneal neovascularization. *Drug Deliv.* 2019;26(1):522–31.
56. Chan PS, Li Q, Zhang B, To KK, Leung SS. In vivo biocompatibility and efficacy of dexamethasone-loaded PLGA-PEG-PLGA thermogel in an alkali-burn induced corneal neovascularization disease model. *Eur J Pharm Biopharm.* 2020;155:190–8.
57. Zhang L, Shen W, Luan J, et al. Sustained intravitreal delivery of dexamethasone using an injectable and biodegradable thermogel. *Acta Biomater.* 2015;23:271–81.
58. Xie B, Jin L, Luo Z, et al. An injectable thermosensitive polymeric hydrogel for sustained release of Avastin® to treat posterior segment disease. *Int J Pharm.* 2015;490(1-2):375–83.
59. Kamali H, Khodaverdi E, Hadizadeh F, Mohajeri SA. In-vitro, ex-vivo, and in-vivo evaluation of buprenorphine HCl release from an in situ forming gel of PLGA-PEG-PLGA using N-methyl-2-pyrrolidone as solvent. *Mater Sci Eng C.* 2019;96:561–75.
60. Xu WK, Tang JY, Yuan Z, et al. Accelerated cutaneous wound healing using an injectable teicoplanin-loaded PLGA-PEG-PLGA thermogel dressing. *Chin J Polym Sci.* 2019;37(6):548–59.
61. El-Zaafarany GM, Soliman ME, Mansour S, et al. A tailored thermosensitive PLGA-PEG-PLGA/emulsomes composite for enhanced oxcarbazepine brain delivery via the nasal route. *Pharmaceutics.* 2018;10(4):217.
62. Feng Y, Wang F, Zhang XW, Bhutani H, Ye B. Characterizations and bioactivities of abendazole sulfoxide-loaded thermo-sensitive hydrogel. *Parasitol Res.* 2017;116(3):921–8.
63. Garner J, Davidson D, Eckert GJ, Barco CT, Park H, Park K. Reshapable polymeric hydrogel for controlled soft-tissue expansion: in vitro and in vivo evaluation. *J Control Release.* 2017;262:201–11.
64. Guo X, Zhu X, Liu D, Gong Y, Sun J, Dong C. Continuous delivery of propranolol from liposomes-in-microspheres significantly inhibits infantile hemangioma growth. *Int J Nanomedicine.* 2017;12:6923.
65. Li X, Chen L, Lin H, et al. Efficacy of poly (D, L-lactic acid-co-glycolic acid)-poly (ethylene glycol)-poly (D, L-lactic acid-co-glycolic acid) thermogel as a barrier to prevent spinal epidural fibrosis in a postlaminectomy rat model. *Clin Spine Surg.* 2017;30(3):E283–90.
66. Huang C, Fu C, Qi ZP, et al. Localised delivery of quercetin by thermo-sensitive PLGA-PEG-PLGA hydrogels for the treatment of brachial plexus avulsion. *Artif Cells Nanomed Biotechnol.* 2020;48(1):1010–21.

67. Kamali H, Khodaverdi E, Hadizadeh F, et al. Comparison of in-situ forming composite using PLGA-PEG-PLGA with in-situ forming implant using PLGA: in-vitro, ex-vivo, and in-vivo evaluation of naltrexone release. *J Drug Deliv Sci Technol.* 2019;50:188–200.
68. Rong X, Ji Y, Zhu X, et al. Neuroprotective effect of insulin-loaded chitosan nanoparticles/PLGA-PEG-PLGA hydrogel on diabetic retinopathy in rats. *Int J Nanomedicine.* 2019;14:45.
69. Wang P, Zhuo X, Chu W, Tang X. Exenatide-loaded microsphere/thermosensitive hydrogel long-acting delivery system with high drug bioactivity. *Int J Pharm.* 2017;528(1-2):62–75.
70. Wang SJ, Qin JZ, Zhang TE, Xia C. Intra-articular injection of kartogenin-incorporated thermogel enhancing osteoarthritis treatment. *Front Chem.* 2019;7:677.
71. Yan Q, Xiao LQ, Tan L, et al. Controlled release of simvastatin-loaded thermo-sensitive PLGA-PEG-PLGA hydrogel for bone tissue regeneration: in vitro and in vivo characteristics. *J Biomed Mater Res A.* 2015;103(11):3580–9.
72. Liu Y, Chen X, Li S, et al. Calcitonin-loaded thermosensitive hydrogel for long-term antiosteopenia therapy. *ACS Appl Mater Interfaces.* 2017;9(28):23428–40.
73. Xu J, Feng Y, Wu Y, et al. Noninvasive monitoring of bone regeneration using NaYF₄: Yb³⁺, Er³⁺ upconversion hollow microtubes supporting PLGA-PEG-PLGA hydrogel. *React Funct Polym.* 2019;143:104333.
74. Li X, Ding J, Zhang Z, et al. Kartogenin-incorporated thermogel supports stem cells for significant cartilage regeneration. *ACS Appl Mater Interfaces.* 2016;8(8):5148–59.
75. Zheng XQ, Huang JF, Lin JL, et al. Controlled release of baricitinib from a thermos-responsive hydrogel system inhibits inflammation by suppressing JAK2/STAT3 pathway in acute spinal cord injury. *Colloids Surf B Biointerfaces.* 2021;199:111532.
76. Chen X, Li F, Feng L, Yu L, Ding J. An injectable Thermogel containing levonorgestrel for long-acting contraception and fertility control of animals. *J Biomed Nanotech.* 2017;13(11):1357–68.
77. Atanasov G, Kolev IN, Petrov O, Apostolova MD. Synthesis of PLGA-PEG-PLGA polymer Nanomicelles—carriers of Combretastatin-like antitumor agent 16Z. In: *Nanoscience and nanotechnology in security and protection against CBRN threats.* Dordrecht: Springer; 2020. p. 449–58.
78. Yang Z, Yu S, Li D, et al. The effect of PLGA-based hydrogel scaffold for improving the drug maximum-tolerated dose for in situ osteosarcoma treatment. *Colloids Surf B Biointerfaces.* 2018;172:387–94.
79. Patel N, Ji N, Wang Y, Li X, Langley N, Tan C. Subcutaneous delivery of albumin: impact of thermosensitive hydrogels. *AAPS PharmSciTech.* 2021;22(3):1–8.
80. Sun J, Lei Y, Dai Z, et al. Sustained release of brimonidine from a new composite drug delivery system for treatment of glaucoma. *ACS Appl Mater Interfaces.* 2017;9(9):7990–9.
81. Lin W, Xu T, Wang Z, Chen J. Sustained intrathecal delivery of amphotericin B using an injectable and biodegradable thermogel. *Drug Deliv.* 2021;28(1):499–509.
82. Mora-Pereira M, Abarca EM, Duran S, et al. Sustained-release voriconazole-thermogel for subconjunctival injection in horses: ocular toxicity and in-vivo studies. *BMC Vet Res.* 2020;16:1–14.
83. Ochin CC, Garelnabi M. Berberine encapsulated PLGA-PEG nanoparticles modulate PCSK-9 in HepG2 cells. *Cardiovasc Haematol Disord Drug Targets (Formerly Current Drug Targets-Cardiovascular & Hematological Disorders).* 2018;18(1):61–70.
84. Ning C, Guo Y, Yan L, et al. On-demand prolongation of peripheral nerve blockade through bupivacaine-loaded hydrogels with suitable residence periods. *ACS Biomater Sci Eng.* 2018;5(2):696–709.